Conformations of Azacyclodeca-3,8-diynes and 1,6-Diazacyclodeca-3,8-diynes and the *Generalized Anomeric Effect*: A Test for Current Conformational Models for Azaheterocycles

Joachim Ritter, Rolf Gleiter,* Hermann Irngartinger, and Thomas Oeser

Contribution from the Organisch-Chemisches Institut der Universität Heidelberg, Im Neuenheimer Feld 270, D-69120 Heidelberg, Germany

Received August 12, 1996. Revised Manuscript Received August 2, 1997[⊗]

Abstract: The conformations of azacyclodeca-3,8-diyne (**4a**) and its *N*-methyl (**4b**) and *N*-isopropyl (**4c**) derivatives as well as 1,6-diazacyclodeca-3,8-diyne (**5a**) and its 1,6-dimethyl (**5b**), 1,6-diisopropyl (**5c**), 1,6-di-*tert*-butyl (**5d**), and 1,6-ditolyl (**5e**) derivatives have been investigated by single-crystal X-ray diffraction, in solution by NMR and by theoretical methods. In the solid state, **4a,c** and **5a**−**e** adopt a chair conformation with the substituents in the bis-axial positions. In solution **4** and **5** show $\Delta G^{\ddagger} = 10.4$ and 11.0 kcal/mol, respectively, for ring inversion. Trapping of **5c** with HCl indicates the presence of bis-axial, axial, and equatorial conformations in solution. The equilibrium between boat and chair conformations in **4** and **5** is ascribed to much reduced *torsional strain* between the propargylic hydrogens. The preference of the axial orientation of the substituents on the nitrogen atom(s) in **4** and **5** is interpreted in terms of the vicinal interactions of both the NR bond and the *lone pair* with the adjacent CH and CC bonds, synaxial 1,3-interactions of both the NR bond and the *lone pair*, and secondary interactions of CH/CC bonds of the alkyl substituent with the endocyclic CH_2 groups as well as with triple bonds (*back* and *front strain*).

Introduction

Conformational preference of N-substituted piperidines (**1**), piperazines (**2**), and related azaheterocycles has been a major topic of conformational analyses since early work from Eliel, Anet, and others showed that exocyclic amine substituents in piperazines and piperidines are found to favor the equatorial rather than the axial position.[1,2] In contrast to this observation 1,3-azacycles (**3**) like tetrahydrooxazines, tetrahydrothiazines, and hexahydropyrimidines prefer an axial orientation of the amine substituent in most cases,[3] implying a gauche position of the N−R axial substituent with respect to the C−X endocyclic bond. This phenomenon is a manifestation of the *generalized anomeric effect*[4] and has been discussed controversely in terms of dipole−dipole interactions,[5] interactions between *lone pairs* (*rabbit ear effect*),[1b] and hyperconjugative interactions.[6,7] The orientational preference of exocyclic amine substituents in **1**−**3** can be considered as a result of two major contributions: (a) vicinal interactions between endocyclic methylene groups and N−R groups as well as *lone pairs* and (b) synaxial 1,3-interactions. To gain further information on the impact of the first contribution, an investigation of model compounds lacking synaxial 1,3-interactions seemed intriguing.

The formal insertion of one triple bond each between the endocyclic C−C bonds in **1** and **2** leads to the "elongated piperidine and piperazine" azacyclodeca-3,8-diyne (**4a**) and 1,6-diazacyclodeca-3,8-diyne (**5a**).[8] The triple bonds in **4** and **5** lead to a total "knock out" of synaxial 1,3-interactions as well as of torsional strain between the endocyclic methylene groups. Therefore our model compounds **4** and **5** allow study of the interactions of lone pairs and their preferred orientation for the first time. In terms of conformational analysis of azacycles this is a new methodological approach. In this paper, we report the conformational properties of **4** and **5**; however, our observations are not restricted on these alkynes. Our study was also designed to provide additional insight into the influence of *lone pair* interactions on conformational properties of cyclic amines. This is directly related to the *generalized anomeric effect*. As

[⊗] Abstract published in *Advance ACS Abstracts,* September 15, 1997.

(1) (a) Harris, R. K.; Spragg, R. A. *J. Chem. Soc. B* **1968**, 684. (b) Hutchins, R. O.; Kopp, D. L.; Eliel, E. L. *J. Am. Chem. Soc.* **1968**, *90*, 7174. (c) Crowley, P. J.; Robinson, M. J. T.; Ward, M. G. *J. Chem. Soc., Chem. Commun.* **1974**, 825. (d) Eliel, E. L.; Vierhapper, F. W. *J. Am. Chem. Soc.* **1975**, *97*, 2424. (e) Appleton, D. C.; McKenna, J.; McKenna, J. M.; Sims, L. B.; Walley, A. R. *J. Am. Chem. Soc.* **1976**, *98*, 292. (f) Anet, F. A.; Yavari, I. *Tetrahedron Lett.* **1976**, *17*, 2093. (g) Anet, F. A.; Yavari, I. *J. Am. Chem. Soc.* **1977**, *99*, 2794.

(2) Reviews: (a) Lambert, J. B.; Featherman, S. I. *Chem. Rev.* **1975**, *75*, 611. (b) Blackburne, I. D.; Katritzky, A. R.; Takeuchi, Y. *Acc. Chem. Res.* **1975**, *8*, 300. (c) Rubiralta, M.; Giralt, E.; Diez, A. *Piperidine*; Elsevier: Amsterdam, 1991. (d) Delpuech J.-J. In *Cyclic Organonitrogen Stereodynamics*; Lambert, J. B., Takeuchi, Y., Eds.; Verlag Chemie: Weinheim, 1992 Chapter 7. (e) Crabb, T. A.; Katritzky, A. R. *Adv. Heterocycl. Chem.* **1984**, *36*, 3.

(3) (a) Allingham, Y.; Cookson, R. C.; Crabb, R. C.; Vary, T. A. *Tetrahedron* **1968**, *24*, 4625. (b) Ferguson, I. J.; Katritzky, A. R.; Read, A. R. *J. Chem. Soc., Perkin Trans. 2.* **1977**, 818. (c) Booth, H.; Lemieux, R. U. *Can. J. Chem.* **1971**, *49*, 777. (d) Jones, R. A. Y.; Katritzky, A. R.; Richards, A. C.; Saba, S.; Sparrow, A. J.; Terpanier, D. L. *J. Chem. Soc., Chem. Commun.* **1972**, 673.

(4) Reviews: (a) Lemieux, R. U. *Pure Appl. Chem.* **1971**, *25*, 527. (b) Szarek, W. A., Horton, D., Eds. *The Anomeric Effect: Origin and Consequences*; ACS Symposium Series; American Chemical Society: Washington, DC, 1979; p 87. (c) Juaristi, E.; Cuevas, G. *The Anomeric Effect*; CRC Press: Boca Raton, FL, 1995. Thatcher, G. R. J. *The Anomeric Effect and Associated Stereoelectronic Effects*; ACS Symposium Series; American Chemical Society: Washington, DC, 1993; Vol. 539. Graczyk, P. P.; Mikolajczyk, M. *Top. Stereochem.* **1994**, *21*, 1389. (d) Eliel, E. L.; Wilen, S. H. *Stereochemistry of Organic Compounds*; Wiley: New York, 1994; pp 740−754.

(5) (a) Edward, J. T. *Chem. Ind.* **1955**, 1102. (b) Kirby, A. J. *The Anomeric Effect and Related Stereoelectronic Effects at Oxygen;* Springer-Verlag: Berlin, 1983. (c) Perrin, C. L.; Armstrong, K. B.; Fabian, M. A. *J. Am. Chem. Soc.* **1994**, *116*, 715. (d) Wiberg, K. B.; Marquez, M. J. *J. Am. Chem. Soc.* **1994**, *116*, 2197.

(6) Romers, C.; Altona, C.; Buys, H. R.; Havinga, E. *Topics in Stereochemistry*; Eliel, E. L., Allinger, N. L., Eds.; Wiley-Interscience: New York, 1969.

(7) Salzner, U. *J. Org. Chem.* **1995**, *60*, 986 and references therein.

(8) (a) Ritter, J.; Gleiter, R. *Liebigs Ann./Recueil* **1997**, 2113. (b) Ritter, J. Dissertation, Universität Heidelberg, 1995.

S0002-7863(96)02825-9 CCC: $14.00

Table 1. Selected Bond Lengths, Transannular Distances (Å), and Bond Angles (deg) of the Azacyclodeca-3,8-diynes **4a**,**c** and the 1,6-Diazacyclodeca-3,8-diynes **5a**−**e**, **6,** and **7**

	bond C(sp)−C(sp)	length C(sp)−C(sp^3)	transannular C(sp)···C(sp)	distance 1···6 (*I*)[a]	bond angle C(sp)−C(sp)−C(sp^3)	pyramidalization of N[b]
6	1.188(1)	1.466(3)	2.991(2)	5.141(2)	171.7(2)	
4a	1.192(1)	1.474(2)	2.978(2)	5.133(2)	170.5(2)	0.347(2)
	1.194(1)	1.472(2)	2.987(2)		170.3(2)	
		1.478(2)			171.8(2)	
		1.477(2)			172.0(2)	
4c	1.190(2)	1.473(2)	2.976(2)	5.128(2)	169.1(2)	0.402(2)
	1.192(2)	1.472(2)	2.984(2)		169.9(1)	
		1.484(2)			171.3(2)	
		1.484(2)			172.0(1)	
5a	1.188(1)	1.482(2)	2.927(2)	5.141(2)	170.7(1)	0.358(2)
		1.478(2)			171.1(1)	
5b	1.190(1)	1.484(1)	2.952(2)	5.137(2)	169.8(2)	0.395(2)
		1.487(2)			170.8(1)	
5c	1.190(2)	1.473(2)	2.959(2)	5.099(2)	168.7(2)	0.412(3)
		1.477(2)			169.9(2)	
5d	1.181(3)	1.487(3)	2.919(3)	5.217(2)	169.7(2)	0.296(3)
		1.484(3)			170.8(3)	
5e	1.172(4)	1.475(4)	2.999(4)	5.002(2)	168.0(3)	0.290(4)
		1.472(4)			170.4(3)	
7	1.189(2)	1.469(2)	2.909(2)	4.935	169.6(1)	

[a] (*I*) Transannular distances between atomic (C, N, O) positions 1 and 6 parallel to the triple bonds. [b] Distance of the N-atom from the plane of the three adjacent C-atoms.

Scheme 1[a]

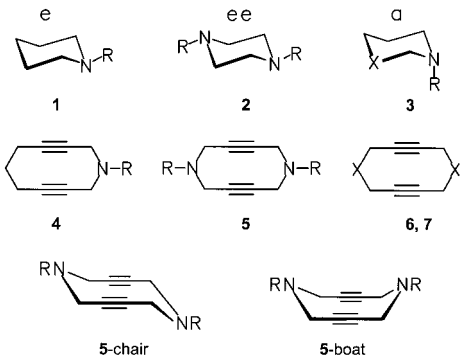

[a] e = equatorial, ee = bis-equatorial, a = axial; **3**: X = O, N, S; **4a**: R = H, **4b**: R = Me, **4c**: R = i-Pr; **5a**: R = H, **5b**: R = Me, **5c**: R = *i*-Pr, **5d**: R = *t*-Bu, **5e**: R = *p*-Tol; **6**: X = CH_2; **7**: X = O.

reported previously[9] we expect similar energies for the chair and boat conformations of **4** and **5** with a preference for the axial conformers. To check these predictions and to find a common explanation for the influence of *lone pair* interactions on cyclic organonitrogen stereodynamics, we have studied the structures of **4a**[8] and **5a**[8] as well as those of their homologues **4c** and **5b**−**e** (**a** = H, **b** = Me, **c** = *i*-Pr, **d** = *t*-Bu, **e** = *p*-Tol)[8] using single-crystal X-ray diffraction and in solution using dynamic NMR spectroscopy and conformational trapping by kinetically controlled protonation.

X-ray Investigations and Theoretical Calculations

Single crystals of the azacyclodeca-3,8-diynes **4a** (R = H) and **4c** (R = *i*-C_3H_7) were obtained by vacuum sublimation at 50 °C and crystallization from $CHCl_3$ solutions at −20 °C, respectively. The X-ray diffraction experiments were performed at 183 K/223 K to avoid thermal decomposition. Compound **4a** crystallizes in the monoclinic space group $P2_1/c$ (Z = 4), and **4c** crystallizes in the triclinic space group $P\bar{1}$ (Z = 2). The structure of **4a** is shown in Figure 1 (top). Structure **4c** is available as Supporting Information. Both structures exhibit a chair conformation with the NH− and N−*i*-C_3H_7 bonds

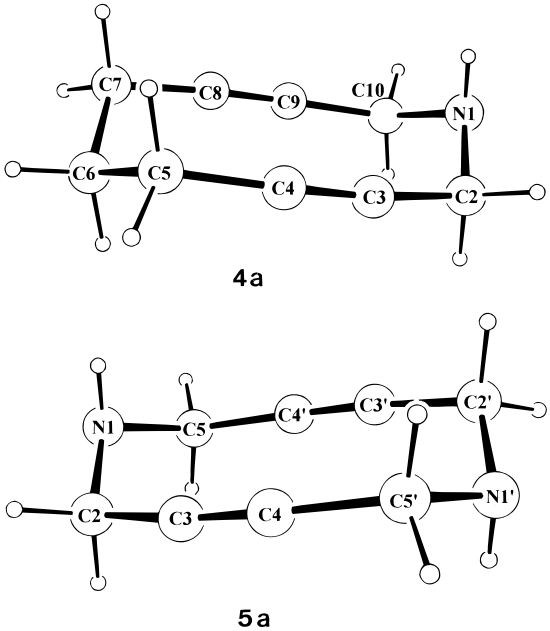

Figure 1. Molecular structures as determined by X-ray analyses of azacyclodeca-3,8-diyne (**4a**) and 1,6-diazacyclodeca-3,8-diyne (**5a**).

orientated axially. The most relevant distances and angles of **4a**,**c** are collected in Table 1 and are compared with the corresponding data published for 1,6-cyclodecadiyne (**6**)[10] and 1,6-dioxacyclodeca-3,8-diyne (**7**).[11] The bond lengths of the triple bonds of **4a,c** (1.190−1.194), the transannular distances between the triple bonds (2.98−2.99 Å), and the angles at the C(sp) centers (169.1−172.0°) are close to the values reported for **6** and **7**. The endocyclic (sp−C(sp^3)) bonds, especially those of the azapropano bridges, are somewhat longer (ca. 0.010−0.020 (Å)) than in **6**.

Semiempirical MO calculations (AM1[12]) as well as Hartree−Fock SCF calculations[15] with a 3-21G* basis predict a preference for the chair conformation with the axial orientation of

(9) Gleiter, R.; Hövermann, K.; Ritter, J.; Nuber, B. *Angew. Chem.* **1995**, *107*, 867.

(10) Gleiter, R.; Karcher, M.; Jahn, R.; Irngartinger, H. *Chem. Ber.* **1988**, *121*, 735.

(11) Gleiter, R.; Rittinger, S.; Irngartinger, H. *Chem. Ber.* **1991**, *124*, 365.

Table 2. Absolute and Relative ΔH_f Values (AM1) as Well as Hartree Energies (3-21G*/6-31G*) of the Axial and Equatorial Chair (**I, II**) and Boat Conformations (**III**, **IV**) of Monoazacyclodecadiynes **4a**−**c** and the 1,6-Diazacyclodeca-3,8-diynes **5a**−**e**

	method	**I** (chair axial)	**II** (chair equatorial)	**III** (boat axial)	**IV** (boat equatorial)
4a	AM1	79.9/**0.0**	86.7/**6.8**	79.8/−**0.1**	87.1/**7.2**
	6-31G*	−251962.1/**0.0**	−251958.5/**3.6**	−251961.9/**0.2**	−251958.4/**3.7**
4b	AM1	83.0/**0.0**	88.0/**5.0**	82.6 /−**0.4**	88.0/**5.0**
	3-21G*	−274923.5/**0.0**	−274916.8/**6.7**	−274923.4/**0.1**	−274916.8/**6.7**
4c	AM1	78.2/**0.0**	83.5/**5.3**	78.3/**0.1**	83.5/**5.3**
	3-21G*	−323641.6/**0.0**	−323632.7/**8.9**	−323641.4/**0.2**	−323632.6/**9.0**
5a	AM1	90.4/**0.0**	103.8/**13.4**	90.6/**0.2**	104.3/**13.9**
	6-31G*	−261987.4/**0.0**	1−261980.2/**7.2**	−261987.0/**0.4**	−261979.6/**7.8**
5b	AM1	96.0/**0.0**	106.2/**10.2**	96.0/**0.0**	106.8/**10.8**
	6-31G*	−310968.3/**0.0**	−310961.1/**7.2**	−310967.6/**0.7**	−310960.6/**7.7**
5c	AM1	87.1/**0.0**	97.2/**10.1**	87.0/−**0.1**	97.6/**10.5**
	3-21G*	−406684.5/**0.0**	−406666.9/**17.6**	−406684.2/**0.3**	−406666.3/**18.2**
5d	AM1	88.2/**0.0**	96.2/**8.0**	89.1/**0.9**	96.4/**8.2**
5e	AM1	176.1/**0.0**	183.6/**7.5**	179.2/**2.9**	184.3/**8.1**

the substituent at the nitrogen atom in both **4a** and **4c** (see Table 2). Similar results were obtained by using the MNDO/2[13] and PM3[14] procedures. It is interesting to note that all four methods anticipate the boat conformation with the nitrogen substituent (R) in the axial position to be about the same energy as the axial chair conformation. The same result is found for the corresponding equatorial species, indicating that not the boat to chair transformation but the inversion of the nitrogen atom has a crucial influence on the total energy of the conformations.

The X-ray investigations on single crystals (from Et_2O or $CHCl_3$ solutions, −20 °C) of **5a**−**e**[16] reveal for all five compounds the chair conformation with all substituents adopting the axial positions solely (monoclinic, C_i symmetry, space groups $P2_1/n$ or $P2_1/c$, two molecules in each unit cell). In Figure 1 (bottom) we show the molecular structure of **5a**. The structures of **5b**−**e** look similar and are provided as Supporting Information. The most relevant bond distances and bond angles are collected in Table 1. As anticipated, the transannular distances between the triple bonds (2.919−2.999 Å) are between those reported for **6** and 1,6-dioxacyclodeca-3,8-diyne (**7**).[11] The cisoid deformation at the sp centers amounts to 8.9−12.0°. As seen for the monoaza compounds, the endocyclic C(sp)−C(sp^3) bonds are slightly longer (ca. 0.010−0.020 (Å)) than in **6**. The pyramidalization varies between 0.290 and 0.412 Å increasing with the donor ability of the exocyclic nitrogen substituent. In the case of the *tert*-butyl derivative **5e** steric effects seem to have a stronger influence.

Quantum chemical calculations on **5a**−**e** with semiempirical methods (AM1[12]) and HF-SCF calculations[15] with a 6-31G* basis for **5a**,**b** and a 3-21G* basis for **5c** predict very similar energies for the bis-axial chair and the bis-axial boat conformations (Table 2). Similar results on **5a**,**b** were obtained with MNDO/2[13] and PM3[14] methods. Regardless, the structure with the highest possible symmetry was found to be the local minimum on the conformational hypersurface. Bis-equatorial boat and chair conformations are always found to be significantly higher in total energy. The difference in energies between bis-axial and mixed axial/equatorial species is exactly one-half of the difference between bis-axial and bis-equatorial conformers. In all cases, the total energy or heat of formation depends mainly on the position of the nitrogen substituents and the *lone pair* orientation, respectively.

(12) Dewar, M. J. S.; Zöbisch, E. G.; Healy, E. F.; Stewart, J. J. P. *J. Am. Chem. Soc.* **1985**, *107*, 3902.
(13) Dewar, M. J. S.; Thiel, W. *J. Am. Chem. Soc.* **1977**, *99*, 4899.
(14) Stewart, J. J. P. *J. Comput. Chem.* **1989**, *10*, 209.
(15) Program SPARTAN: Hehre, W. J.; Burker, L. D.; Shusterman, A. J.; Pietro, W. J. Wavefunction, Inc., Irvine, CA, 1995.
(16) Gleiter, R.; Ritter, J.; Irngartinger, H.; Lichtenthäler, J. *Tetrahedron Lett.* **1991**, *32*, 2887.

Solution Investigations

Compounds **1** and **2** adopt chair conformations[17] in solution and in the gas phase. At room-temperature fast ring (I_R) and nitrogen inversion (I_N) interconverts all axial and equatorial positions. Assuming the equatorial and axial substituents (e_i, a_i) to be nonidentical both dynamic processes lead to four different conformers which are generally rapidly interconverting with each other. The free activation enthalpies of these processes for **1a,b** and **2a,b** are $\Delta G^{\ddagger} = 11-13$ kcal/mol (I_R) and $\Delta G^{\ddagger} = 4-6$ kcal/mol (I_N),[1a,c,f,g,18] respectively. The standard free energies for the equatorial/axial equilibrium are 0.4 kcal/mol in the case of **1a**[1g,2b] and 2.7 kcal/mol for **1b**[1e,19] with the equatorial species being the more stable in both cases.

NMR Investigations and Used Formulas[2d,20]

As in the case of piperidine, dynamic NMR spectroscopy and conformational trapping were used to investigate the inversion processes of **4** and **5**. Important quantities for dynamic NMR spectroscopy are the lifetime τ of a conformer which is equal to

$$^1/_2\pi\Delta\nu \geqslant \tau = 1/k \qquad (1)$$

where $\Delta\nu$ is the difference of the resonance frequences of two exchanging nuclei. For geminal exchanging protons A and B with a coupling constant ^2J, the rate k_c at the coalescence temperature T_c amounts to

$$k_C = 2.22(\Delta\nu^2 + 6J_{AB}{}^2)^{1/2} \qquad (2)$$

This gives

$$\Delta G^{\ddagger}_C = 4.58T_C[10.32 + \log(T_C/k_C)]\ (\text{cal/mol}) \qquad (3)$$

The conformational equilibria in **4** and **5** are more complex than in **1** and **2** because boat conformations also have to be considered. For entropic reasons a direct inversion of boat or chair conformation is less likely than a half-ring inversion

(17) (a) Ansel, G. B.; Burkard, L. A.; Finnegan, W. G. *Chem. Commun.* **1969**, 459. (b) Buckley, P. J.; Constain, C. C.; Parkin, J. E. *Chem. Commun.* **1968**, 668. (c) Blackburne, I. D.; Duke, R. P. K.; Jones, R. A. Y.; Katritzky, A. R.; Record, K. A. F. *J. Chem. Soc., Perkin Trans. 2* **1973**, 332. (d) Lambert, J. B.; Featherman, S. I. *Chem. Rev.* **1975**, *75*, 611.
(18) (a) Baldock, R. W.; Katritzky, A. R *J. Chem. Soc. B* **1968**, 1470. (b) Gittins, V. M.; Heywood, P. J.; Wyn-Jones, E. J. *J. Chem. Soc., Perkin Trans. 2* **1975**, 1642. (c) Lambert, J. B.; Keske, R. G.; Carhart, R. E.; Jovanovich, A. P. *J. Am. Chem. Soc.* **1967**, *89*, 3761.
(19) Crowley, P. J.; Robinson, M. J. T.; Ward, M. G. *Tetrahedron* **1977**, *18*, 915.
(20) Reference 2d, Chapter 7.1.4, 7.2. Friebolin, H. *One- and two-dimensional NMR−Spectroscopy*; VCH: Weinheim, Germany, 1992.

Scheme 2. Half-Ring Inversion I_R* and Nitrogen Inversion I_N for 1,6-Diazacyclodeca-3,8-diynes (only four out of 16 structures are shown)

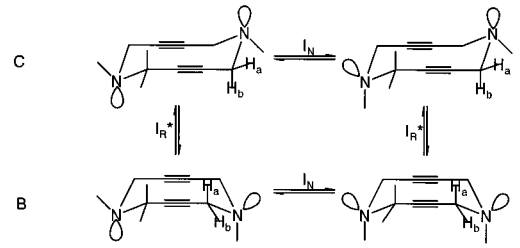

process I_R* as shown in Scheme 2 for **5**. The half-ring inversion process I_R* is different from the ring inversion I_R found in piperazines (where the boat is a transition state) since a conformation with a different symmetry (boat) is found after one single I_R* process. In the full scheme (see Supporting Information), 16 different species are related to each other by I_N (rows) and I_R* (columns). The axial (H_a) and equatorial (H_e) hydrogen atoms will appear as a single resonance in the ^{1}H NMR only if both I_R* and I_N are fast on the NMR time scale, i.e., (H_a) and (H_e) interconvert rapidly with each other. A twist boat form was not found to be a local minimum on the conformational hypersurface (force field, AM1, PM3, ab initio calculations). The theoretical results suggest strong $\pi-\pi$ interactions being the main reason for the instability of twist boat conformations.

At room temperature, the ^{1}H NMR spectrum (CD_2Cl_2) of the dimethyl derivative **5b** exhibits only two resonances, one signal for the ring protons ($\delta = 3.49$) and one for the methyl protons ($\delta = 2.52$). Similarly the ^{13}C NMR spectrum also exhibits one resonance for the sp^3 ring carbon atoms ($\delta = 46.6$) and one signal for the CH_3 group ($\delta = 39.9$). The resonance of the alkyne carbon atoms is found at $\delta = 82.5$. Lowering the temperature leads to a broadening of the ^{1}H NMR CH_2 signals at $\delta = 3.49$. This broadening is due to retardation of the half-ring inversion (I_{R*}) process (Scheme 2). The coalescence temperature T_C for the half-ring inversion process is 230 K (−43 °C) (Figure 2). Similarly the methyl signal displays coalescence at 216 K (−59 °C).

Further temperature lowering to 193 K (−80 °C) leads to decoalescence to five signals in the ^{1}H NMR spectrum at $\delta = 3.2-3.7$ and two signals centered at $\delta = 2.5$. According to these results at temperatures below T_C, two sets of diastereomers can be discriminated, the chair conformers **C** and the boat ones **B** (see Scheme 2). Due to I_R* being slower than I_N an AA′BB′ pattern for the diastereomeric ring protons is observed separately for boat and chair conformers. Superposition of the two AA′BB′ subspectra (AA′BB′$_{(1)}$, AA′BB′$_{(2)}$) of different intensities and slow-exchange-limit frequency separation ($\delta\nu$) results in the pattern observed between $\delta = 3.2-3.7$. From the variable temperature ^{1}H NMR data (Table 3), we can derive a free activation enthalpy $\Delta G^{\ddagger}$ of 10.7−11.0 kcal/mol. At 193 K, the methyl signals of both conformers are separated and an equilibrium constant of $K_R = 1.3 \pm 0.1$ was measured.

Our assumption that the boat is the preferred conformation in solution is based on the higher average dipole moment of the C_{2v} symmetric boat since polar solvents such as CD_2Cl_2 should stabilize the conformer with a higher dipole moment. AM1 calculations result in a calculated dipole moment near zero for bis-axial and bis-equatorial chair conformers, while for the boat conformers, 0.72/2.20 D (**5b**) and 0.98/2.36 D (**5c**) are calculated. The higher differences in dipole moments for the isopropyl derivative conformers of **5c** compared to the methyl compound **5b** result in the higher diastereomeric ratio observed for **5c**.

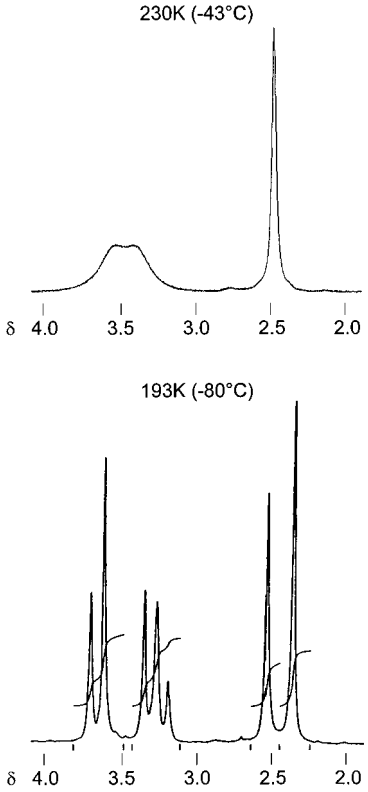

Figure 2. Low-temperature ^{1}H NMR spectra of **5b** (200 MHz, CD_2Cl_2, 0.06 mol/L).

Although the AA′BB′ subspectra seem to display two different coupling constants (14 and 16 Hz), an unequivocal assignment to either the boat or the chair conformation is difficult due to strong overlap of the signals. For 1,6-bridged 1,6-diazacyclodeca-3,8-diynes[9] (fixed boat conformation) a geminal coupling constant of $^2J = 16.2$ Hz was found.

The interpretation as a result of boat/chair coexistence is supported by ^{13}C NMR spectra which display two broad (C (sp), CH_3) and one unchanged sharp CH_2 resonance at 213 K evidence for the slow exchange rate for the I_R* process on the ^{13}C NMR time scale. At 203 K two signals for the CH_3 and C (sp) carbon atoms are observed while the resonance of the CH_2 carbon atoms remains unchanged (Table 3). Furthermore, the NMR data recorded for **5c** (Table 3) are consistent with the results obtained for **5b,** but the diastereomeric ratio is four to five times larger. In the case of the parent system **5a,** dynamic NMR analysis was not possible due to its poor solubility at low temperatures in suitable solvents.

To analyze the possible inversion processes in **4b** we assume that in addition to the nitrogen inversion two independent half-ring inversion processes, I_R*(N) and I_R*(C), interconvert the chair and the boat conformers. The processes, I_R*(N), I_R*(C), and I_N, give a set of eight equilibrating structures (Scheme 3). In contrast to **5b**, where the ring inversion process is degenerate, we expect for **4b** a higher activation energy for the ring inversion at nitrogen (I_R*(N)) than for I_R*(C). This assumption is based on ^{1}H as well as ^{13}C NMR investigations on 1,6-cyclodecadiyne (**6**), which shows a coalescence temperature in CD_2Cl_2 below 175 K; however, a full investigation of the signal pattern at 175 K was not possible since the inversion process is still too fast. One might argue that the lower T_c for cyclodeca-1,6-diyne does not necessarily refer to a lower $\Delta G^{\ddagger}$, if the slow-exchange-limit frequency separation ($\Delta\nu$) is smaller than for **4** or **5**. However, even if $\Delta\nu$ is only 40 Hz for cyclodeca-1,6-diyne and $T_c = 175$ K (in fact, T_c is below 175 K since only line broadening was observed), the activation barrier amounts to only

Table 3. ^{2}H NMR Data for **5b**,**c**[a]

	T (K)	^2J (Hz)	$\delta\nu$ (Hz)	T_c (K)	k_C (s^{-1})	$\Delta G^{\ddagger}_C$ (kcal/mol)	K_R	K	ΔG (kcal/mol)
				Compound **5b**					
^{1}H NMR									
CH_2 (AA′BB′$_{(2)}$)	193	14−16	71 ± 4	230 ± 4	178 ± 10	11.0 ± 0.3	1.3 ± 0.1[b]	1.2 ± 0.1[c]	−0.10 ± 0.03[b]
CH_2 (AA′BB′$_{(1)}$)	193	14−16	85 ± 4	230 ± 4	206 ± 10	10.9 ± 0.3			0.10 ± 0.03[b]
CH_3	193		34 ± 2	216 ± 4	75 ± 5	10.7 ± 0.2	1.3 ± 0.1[b]		0.10 ± 0.02[b]
^{13}C NMR									
C(alkyne)	203		35 ± 8	213 ± 5	78 ± 17	10.5 ± 0.4	≈1.6[d]		≈0.2[d]
CH_3	203		56 ± 8	218 ± 5	124 ± 18	10.6 ± 0.3	≈1.5[d]		≈0.15[d]
				Compound **5c**					
^{1}H NMR									
CH_2 (AA′BB′)	193	17.5 ± 1	26 ± 4	208 ± 5	111 ± 10	10.1 ± 0.3	n/a	n/a	n/a
CH	193		22 ± 4	n/a	n/a	n/a	6.0 ± 1[b]		0.7 ±0.1[b]
^{13}C NMR									
C(alkyne)	193		40 ± 5	208 ± 6	89 ± 10	10.2 ± 0.3	≈6[b]		≈0.7[b]

[a] Slow-exchange-limit temperature, T; geminal coupling constants, ^2J; ^{1}H NMR and ^{13}C NMR slow-exchange-limit frequency separation of the resonances of chair and boat at T, T_c; rate constants for I_R*, k_C; free activation enthalpy, $\Delta G^{\ddagger}_C$; thermodynamic equilibrium constant, K_R = [boat]/[chair]; kinetic equilibrium constant, $K = k_{C2}/k_{C1}$; free reaction enthalpy for I_R*, ΔG. [b] 193 K. [c] 230 K. [d] 203 K.

Scheme 3. Half-Ring Inversions I_R*(N) and I_R*(C) and Nitrogen Inversion I_N for **4b**

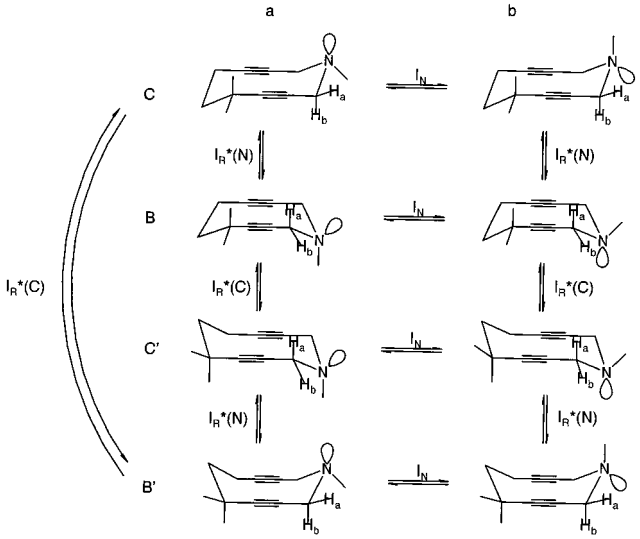

8.4 kcal/mol whereas for **5b** ($\Delta\nu$ = 84 Hz) 11 kcal/mol was found. The ^{1}H NMR investigations of **4b** in CD_2Cl_2 determined a coalescence temperature of 218 K which supports the above assumption. Below 218 K a single AA′BB′ resonance is observed for the CH_2N protons (Figure 3), as the second ring inversion process I_R*(C) is still fast on the ^{1}H NMR time scale and the equilibrium between chair and boat is not resolved.

The data obtained by these investigations of **4b** are collected in Table 4 and compared with those for **5b**,**c**. It is interesting to note that the $\Delta G^{\ddagger}$ value obtained for the monoaza compound **4b** (10.4 kcal/mol) is very similar to that of **5b** (10.7−11.0 kcal/mol). This provides further evidence for the half-ring inversion process I_R*(N) independently active at each endocyclic azapropano unit. As anticipated in the ^{13}C NMR spectrum, only one set of signals is observed since boat and chair conformations are in fast equilibrium due to the I_R*(C) process. At 183 K, strong broadening is observed for the ^{13}C NMR resonance of the central CH_2 carbon atom nearby 25 ppm and it is difficult to accurately determine the coalescence region. This is a result of the retardation of the I_R*(C) process. (The corresponding spectra are provided as Supporting Information).

Conformational Trapping by Fast Protonation

The protonation of the nitrogen atom in amines in strongly concentrated Broensted acids is known to be faster than nitrogen inversion by several orders of magnitude. The product ratio of diastereomeric dihydrochlorides may reflect quantitatively the chemical equilibrium of conformers in the free base if the following conditions are given:[21] Low pH values to guarantee a kinetically controlled reaction and sufficiently low concentrations of free amine to avoid any local pH increase during the protonation reaction. Moreover, retention of configuration

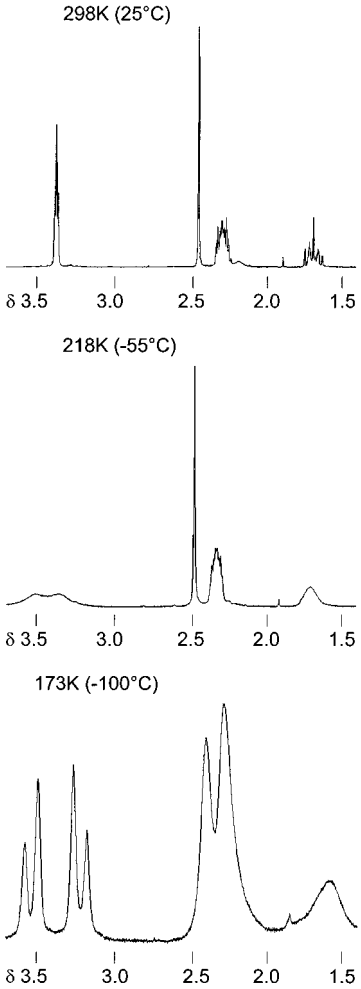

Figure 3. Variable-temperature ^{1}H NMR spectra of **4b** (200 MHz, CD_2Cl_2, 0.06 mol/L).

(21) (a) Booth, H. *Chem. Commun.* **1968**, 802. (b) McKenna, J.; McKenna, J. M. *J. Chem. Soc. B* **1969**, 644. (c) Crowley, P. J.; Morris, G. A.; Robinson, M. J. T. *Tetrahedron Lett.* **1976**, *17*, 3575.

Table 4. $^2H-^1H$ NMR Data of **4b** Compared with Those for **5b**,**c**[a]

compound	T (K)	^2J (Hz)	$\delta\nu$ (Hz)	T_c (K)	k_C (s^{-1})	$\Delta G^{\ddagger}_C$ (kcal/mol)
4b	183	17.5 ± 1	64 ± 3	218 ± 3	171 ± 9	10.4 ± 0.2
5b	193	14−16	71/85 ± 4	230 ± 4	178/206 ± 10	11.0/10.9 ± 0.3
5c	193	17.5 ± 1	26 ± 4	208 ± 5	111 ± 10	10.1 ± 0.3

[a] Slow-exchange-limit temperature, T; geminal coupling constants, ^2J; ^1H NMR slow-exchange-limit frequency separation of the geminal proton resonances at T, T_c; rate constant for I_R*(N), k_C; free activation enthalpy, $\Delta G^{\ddagger}_C$.

during the protonation and the possibility to distinguish the protonated species by NMR is required. Kinetically controlled amine protonation of piperidines and piperazines was realized successfully providing data according to corresponding VT NMR results.[1a,e,f,22]

While in the case of dialkylpiperazines (**2**) bis-equatorial (ee) (>99%) and bis-axial (aa) (<0.5%) conformers give *trans*-dihydrochlorides and mixed conformers (ae and ea, < 1%) *cis*-dihydrochlorides exclusively, the situation for *N*,*N*′-dialkyl-1,6-diazacyclodeca-3,8-diynes (**5**) is somewhat more complicated. As outlined in Scheme 4, pure **5**(aa) or **5**(ee) as well as mixed conformers **5**(ea) and **5**(ae) should give either **5**-*trans*$^{2+}$ or **5**-*cis*$^{2+}$ depending on whether the boat or the chair conformation is protonated. Hence without further assumptions, the ratio of both diastereomeric ammonium ions gives no information about the ratio of the bis-axial, bis-equatorial, and mixed conformers in solution: boat and chair conformations with identical geometries of the nitrogen atoms lead to different dihydrochlorides due to their different overall symmetry.

In the case of a kinetically controlled protonation one obtains the ratio of diastereomers R_D by eq 4. Additionally the equilibrium constant K_R between the boat and the chair conformers is expressed by eq 5. Assuming that the ratio (γ) between the bis-axial/equatorial conformers and mixed conformers is about the same for both chair and boat[23] (see eqs 6 and 7), eq 4

$$R_D = \frac{[\mathbf{5}\text{-}cis^{2+}]}{[\mathbf{5}\text{-}trans^{2+}]} = \frac{[C] + [B]}{[A] + [D]} \tag{4}$$

$$K_R = \frac{[C] + [D]}{[A] + [B]} \tag{5}$$

$$\gamma = \frac{[C]}{[D]} = \frac{[A]}{[B]} \qquad [C] = [D]\gamma \qquad [A] = [B]\gamma \tag{6}$$

$$K_R = \frac{[D]}{[B]} \tag{7}$$

$$R_D(\gamma) = \frac{K_R\gamma + 1}{K_R + \gamma} \tag{8}$$

can be simplified to the form of eq 8. The dependence of the diastereomeric ratio $R_D(\gamma)$ on the boat−chair equilibrium constant K_R and γ is graphically shown in Figure 4, revealing that only for higher K_R values a significant influence of γ on R_D is expected.

Scheme 4. Fast Protonation of All Possible Boat and Chair Conformers of a 1,6-Diazacyclodeca-3,8-diyne (**5**) Results in Formation of Dications **5**-*trans*$^{2+}$ and **5**-*cis*$^{2+}$ [a]

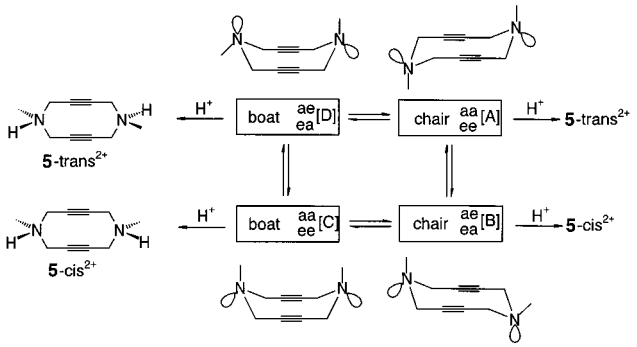

[a] C = chair, B = boat , aa = bis-axial, ae/ea = axial−equatorial, ee = bis-equatorial. [A] = [Caa] + [Cee]; [B] = [Cae] + [Cea]; [C] = [Baa] + [Bee]; [D] = [Bea] + [Bae].

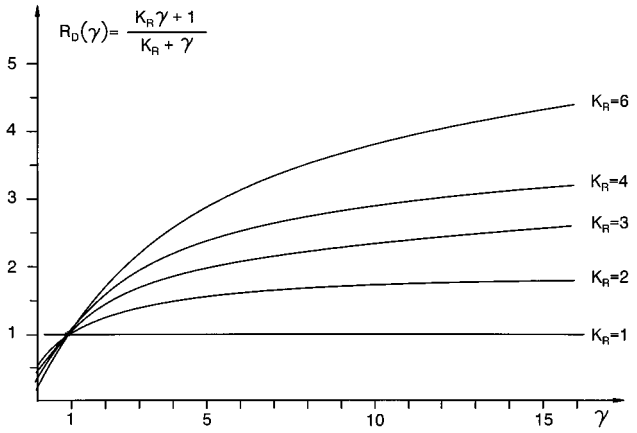

Figure 4. Drawings of the function $R_D(\gamma)$ for different K_R values.

Four cases should be considered in principle:

(a) A small concentration of the bis-axial and bis-equatorial conformers whereas mixed conformers are supposed to be favored. Then $R_D(\gamma)$ goes to $1/K_R$.

$$\lim_{\gamma\to 0} R_D(\gamma) = 1/K_R \tag{9}$$

(b) A high preference for the bis-equatorical conformers gives eq 10, where the approximated value for $R_D(\gamma)$ is closely related to K_R, determined by NMR experiments reported above.

$$\lim_{\gamma\to\infty} R_D(\gamma) = (K_R\gamma)/\gamma = K_R \tag{10}$$

(c) A high preference for the bis-axial species leading to the same result as in case b.

(d) For $R_D(\gamma) \approx 1$, one obtains $\gamma = 1$, indicating a small energy difference between the conformers.

$$\lim_{\gamma\to 1} R_D(\gamma) = 1 \tag{11}$$

The energy diagram for d is given in Figure 5.

(22) (a) Anet, F. A.; Yavari, I.; Ferguson, I. J.; Katritzky, A. R.; Moreno-Manas, M.; Robinson, M. J. T. *Chem. Commun.* **1976**, 399. (b) Delpuech, J.-J.; Martinet, Y. *Tetrahedron* **1972,** *28*, 1759. Delpuech, J.-J.; Deschamps, M.-N. *Tetrahedron* **1978,** ***34***, 3017. (c) Anet, F. A.; Yavari, I. *Tetrahedron Lett.* **1976**, *17*, 2093. (d) Reference 2d and references therein.

(23) Due to the fact that the axial/equatorial equilibrium should be influenced mainly by vicinal interactions between *lone pairs* and methylene groups and not by the chair or boat skeleton as shown by quantum chemical calculations (Table 2).

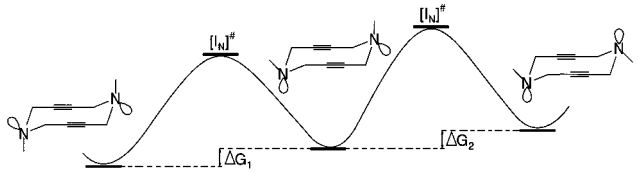

Figure 5. Possible nitrogen inversion (I_N) energy diagram for chair conformations of *N,N′*-dialkyl-1,6-diazacyclodeca-3,8-diynes according to frontier value considerations for $\Delta G_{1/2} < 1$ kcal/mol, $R_D(\gamma) \approx 1$.

If $R_D(\gamma)$ is found to be close to 1, bis-axial and mixed conformers should have similar concentrations, while if $R_D(\gamma)$ is closer to K_R, the bis-axial species should predominate. For this reason kinetic trapping experiments were performed with **5c** ($K_R \approx 6$) rather than **5b** ($K_R = 1.3$). In our trapping experiment we added slowly a solution of **5c** in dry methanol to a saturated methanolic solution of dry HCl at 0 °C. The ^{13}C NMR spectrum of the dihydrochlorides in CF_3COOD shows two isomers. The ^1H NMR spectrum confirms these results, although a definitive assignment of **5c**-*trans*$^{2+}$ and **5c**-*cis*$^{2+}$ is not possible. The ratios of the ^{13}C NMR resonances suggest a $R_D(\gamma)$ value of 1.5 (see Supporting Information). In a second experiment, the protonation was carried out with DCl/D_2O (40%) by adding a diluted solution of **5c** in cyclohexane with vigorous stirring. The ^1H NMR spectrum of the acidic phase shows two superimposed AA′BB′ patterns attributed to the different CH_2 groups and two sets of heptets and doublets for the two different isopropyl groups. Integration gives a diastereomeric ratio of the dihydrochlorides as $R_D(\gamma) = 1.3 \pm 0.2$ (see Supporting Information). Protonation with DCl/D_2O (10%) did not affect the diastereomeric ratio.

Both results provide evidence for the presence of both bis-axial and mixed conformers in similar concentrations. Therefore, the energy difference between aa and ae free base conformers should be less than 1 kcal/mol.

Discussion

We have found a large difference in the conformational preference of compounds **4** and **5** relative to those known for **1** and **2**. In the diynes **4** and **5** we encounter an equilibrium between chair and boat conformations at room temperature in solution and in the solid state and a preference for the axial orientation of the substituents at the nitrogen atom(s). Due to the unique appearance of bis-axially orientated NR groups in the solid state, the bis-axial conformation must have a reasonable concentration in solution.

The equilibrium between boat and chair conformations in **4** and **5** we ascribe to the fact that the *torsional strain* between the propargylic hydrogens is minute.

The preference for the axial orientation of the substituents at the nitrogen(s) in **4** and **5** can be explained in terms of three contributions: (1) vicinal interactions of both the NR bond and the *lone pair* with the adjacent CH and CC bonds;

(2) synaxial 1,3-interactions of both the NR bond and the *lone pair* (Figure 8, top).; and (3) secondary interactions between CH/CC bonds of the alkyl substituent and the endocyclic CH_2 groups as well as with triple bonds (*back and front strain effects*; Figure 8, bottom).

The parent compounds **4a** and **5a** are exceptions as hydrogen substituents show no *back strain* effects with endocyclic CH_2 groups, providing additional information about the competitive importance of *back strain* effects and vicinal interactions.

Crucial differences between axial and equatorial conformations are found in terms of different interactions of the nitrogen *lone pairs* in the two conformers.

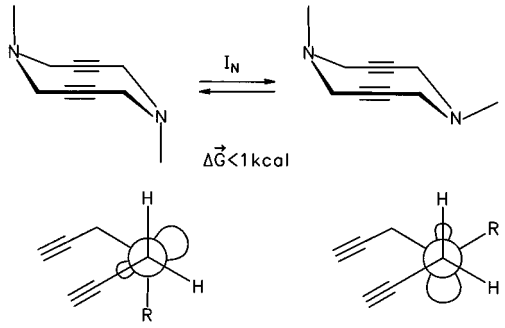

Figure 6. Nitrogen inversion at **5b** and the corresponding vicinal interactions of the lone pairs for axial (left) and equatorial (right) orientation.

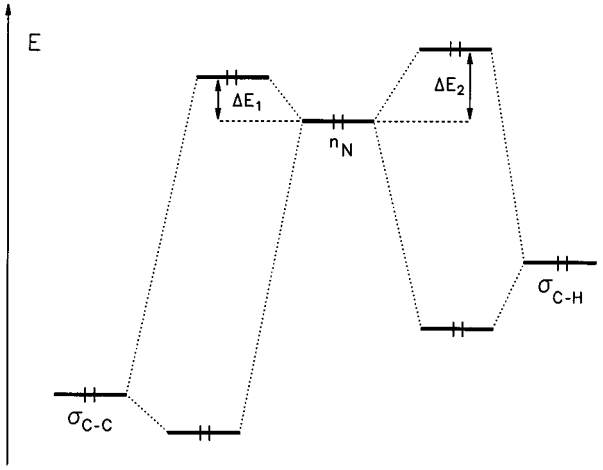

Figure 7. Qualitative MO diagram for $n_N-\sigma_{CH}$ and $n_N-\sigma_{CC}$ hyperconjugation.

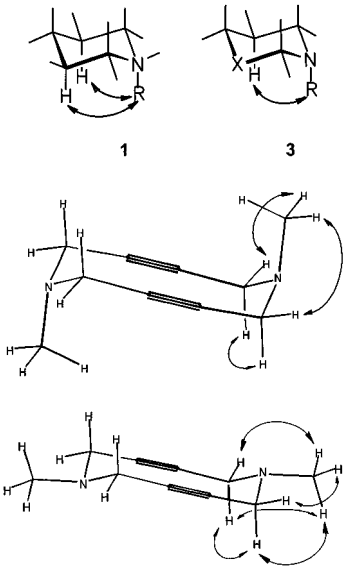

Figure 8. Synaxial 1,3-interactions of axial amine substituents in piperidine (**1**) and **3** (top) and different *back-strain effects* in axial and equatorial conformers of **5b** (bottom).

The axial orientation of the substituents at the nitrogen atoms in **5** (Figure 6, left) causes a gauche arrangement between the *lone pair* at the nitrogen atoms and the propargylic CH_2 groups and an anti arrangement with the CC σ-bond.

In the case of an equatorial orientation of the substituents on the nitrogen atoms in **5** (Figure 6, right), the adjacent axial CH bonds and the nitrogen *lone pairs* show an anti arrangement, whereas lone pairs and endocyclic CC bonds are gauche. In both conformations an antibonding anti interaction of either the

endocyclic CC bonds or the CH bonds with both nitrogen *lone pairs* occurs. Competitive interaction depending on the strength of *lone pair* CH σ-bond hyperconjugation and on the *lone pair* CC σ-bond hyperconjugation on the other hand should have major influence on the preference for axial or equatorial orientation of the nitrogen substituent and the *lone pair*, respectively.

Usually hyperconjugation between nitrogen *lone pairs* and CH bonds is stronger than between CC bonds due to a smaller energy difference[24] between *lone pairs* and CH bonds (Figure 7). Exceptions can be found in highly strained systems.

Therefore the *lone pairs'* preference to occupy the equatorial position (in axial conformations) is an expected result upon further consideration. In the six-membered heterocycles such as **1** and **2** these antibonding hyperconjugative effects are overruled by strong synaxial 1,3-interactions between NR− and axial CH bonds forcing the nitrogen substituent R into the equatorial position. An exchange of the β-CH_2 groups in piperidine with heteroatoms (X = O, S, NMe) diminishes these interactions (Figure 8, top), resulting in the preference of an axial orientation of the methyl group (*generalized anomeric effect*).

In the case of **4** and **5** such synaxial 1,3-interactions are not present since both positions are occupied by triple bonds instead of CH_2 groups and through-space interactions between *lone pairs* and triple bonds in **4** or **5** are small.[8]

Back strain effects should also favor the axial conformation. In Figure 8 (bottom) the synaxial 1,3-interactions between exo- and endocyclic CH bonds are shown for the bis-axial conformer and the bis-equatorial conformer of **5b**. Whereas for the bis-equatorial arrangement five repulsive synaxial 1,3 interactions are encountered, the bis-axial arrangement shows only three. In the axial conformation two weaker synaxial 1,3-interactions between exocyclic CH and endocyclic CC bonds replace two strong synaxial 1,3-interactions between endo- and exocyclic CH bonds, resulting in decreased strain (this is due to the fact that repulsion between bonding orbitals of similar energy is usually stronger[24]). Thus these *back strain* effects also favor the bis-axial conformation; however, we do not believe that this is a crucial factor since **4a** and **5a** which also exhibit the (bis)-axial structure in the solid state have similar $\Delta\Delta H_f$ values compared to the methyl derivatives for the difference between bis-axial and bis-equatorial conformations according to the AM1, MNDO, and ab initio 6-31G* calculations.

Generalized Anomeric Effect and $n_N-\sigma_{CH}$, $n_N-\sigma^*$ Hyperconjugation

We emphasize that our observations are not restricted to **4** and **5**. The well-known conformational properties of **1**−**3** are consistent with our findings. The results for **4** and **5** provide evidence that both vicinal hyperconjugative interactions between *lone pairs* and CH bonds as well as synaxial 1,3-interactions of axial ring substituents should be crucial parameters for the preferred orientation of *lone pairs* in compounds such as **1**−**5** and therefore important for the origin of the *generalized anomeric effect* in **3**.[4,5]

Additional evidence for our conclusions can be derived from X-ray diffraction data of 1,8-diisopropyl-1,8-diazacyclotetradeca-4,11-diyne (**8**).[25] In contrast to **4** and **5** there are strong 1,3-interactions between NR and β-CH_2 groups in the axial conformation of **8**. Consequently, the bis-equatorial conformer was found in the crystalline state as in the case of piperazine.

In the case of six-membered N-heterocycles containing exo- or endocyclic C−X bonds hyperconjugative $n_N - \sigma^*_{CX}$ (X = OR, N, Cl) interactions have also been reported to stabilize conformations where a sufficient overlap between n_N and σ^*_{CX} is possible (e.g., **3**).[7,26,27] This kind of stabilization demands "low-energy" σ^* orbitals and "high-energy" occupied orbitals which means that X should have a distinctly higher electronegativity than carbon.[28] Despite the fact that the C(sp)−C(sp^3) bonds in X-ray structures of **4** and **5** are slightly elongated compared to the carbocyclic **6,** which might be an indication for $n_N-\sigma^*_{C(sp)-C(sp3)}$ interaction, we do not believe them to be crucial. Neither open shell/closed shell AM1 nor HF-6-31G* HF-6-31G*-MP2 calculations indicate a distinct $n_N-\sigma_{CC}$ interaction in bis-axial conformations (based on the α_C AO coefficients) while antibonding interaction between the *lone pair* and α-CH orbitals is strong in equatorial conformations. We attribute this to the fact that the energy gap between n_N and σ^*_{CC} is too large. One might argue that $n-\sigma^*$ interactions might be as important as $\sigma_{CH}-n$ interactions. Our calculations show that there is no evidence that $n-\sigma^*$ interaction is crucial since a significant $n-\sigma^*sp-sp^3$ interaction was not found (based on the AO coefficients). In addition, if $n-\sigma^*$ $sp-sp^3$ interaction would be more important than n-CH hyperconjugation, this bond length should increase steadily from **5a** to **5d** with increasing energy of the nitrogen lone pair. This is not the case. Small *front strain* effects between the out-of-plane π system and the axial nitrogen substituent can cause elongation of the propargylic bonds in some cases.

Conclusion

Our investigations of "elongated" piperazines and piperidines aza- (**4**) and 1,6-diazacyclodeca-3,8-diynes (**5**) provide evidence which indicates that competitive synaxial 1,3-interaction and *lone pair* α-CH hyperconjugative destabilization are crucial for the preference of axial or equatorial conformers in six-membered N-heterocycles. In any case, axial *lone pairs* cause repulsive hyperconjugation with vicinal axial C−H bonds. In the absence of strong synaxial 1,3-interactions of the amine substituent, conformers with equatorially orientated nitrogen *lone pairs* and axial amine substituents are favored. In the presence of vicinal endocyclic CX bonds, as in hexahydrooxazines and -pyrimidines additional hyperconjugative $N_n - \sigma^*_{(CX)}$ interactions should increase the observed preference. We believe that the *generalized anomeric effect* is a result of both types of hyperconjugative interactions and competitive synaxial 1,3-interaction with the relative contribution of these interactions depended upon the steric, structural, and electronic properties of the system. Moreover, we have shown that separation of adjacent CH_2 groups in six-membered rings by introducting triple bonds leads to a local energy minimum for the boat conformation which is as stable as the chair.

Experimental Section

The preparation of **4a**−**c** and **5a**−**e** has been described in the literature.[8]

Trapping Experiments. Our trapping experiments were carried out under the same conditions used for piperazines and piperidines and where the Curtin-Hammet principle does not apply[1c,f] by extracting a

(24) Hoffmann, R.; Radom, L.; Pople, J. A.; Schleyer, P. v. R.; Hehre, W. J.; Salem, L. *J. Am. Chem. Soc.* **1972**, *94*, 6221.

(25) Gleiter, R.; Wolfart, V. *Tetrahedron Lett.* **1996**, *37*, 479.

(26) (a) Salzner, U.; Schleyer, P. v. R. *J. Org. Chem.* **1994**, *59*, 2138. (b) Salzner, U. *J. Org. Chem.* **1995**, *60*, 986.

(27) Anet, F. A.; Kopelevich, M. *Chem. Commun.* **1987**, 595. Forsyth, D. A.; Hanley, J. A. *J. Am. Chem. Soc.* **1987**, *109*, 7930. Forsyth, D. A.; Prapansiri, V. *Tetrahedron Lett.* **1988**, *29*, 3551.

(28) Strong interactions were found in α-fluoroamines and α-fluorocarbanions, for instance: Schleyer, P. v. R.; Kos, A. J. *Tetrahedron* **1983**, *39*, 1141.

diluted solution in an inert immiscible solvent ($c < 0.2$ m) with an excess of a strong acid. A second experiment using methanol instead of cyclohexane as a solvent was performed to see whether a trapping experiment under homogeneous conditions leads to different results.

(a) Trapping experiment in cyclohexane: A solution of **5c** (0.02 m, 80 mg in 20 mL of cyclohexane, 295 K) was dropwise added to a mixture of 10 mL of DCI/D_2O (40%) and 20 mL of cyclohexane under vigorous stirring over a period of 1.5 h. The D_2O layer was separated and immediately investigated by NMR spectroscopy.

(b) Trapping experiment in methanol: At 273 K a methanolic solution of **5c** (0.05 m, 110 mg in 10 mL of dry MeOH) was added dropwise to 50 mL of a saturated methanolic solution of dry HCl over a period of 1.5 h. The white precipitate was separated by utilizing a centrifuge and dried in vacuo (298 K), giving a white powder. This mixture of diastereomeric dihydrochlorides was dissolved in neat CF_3-COOD under dry conditions and immediately investigated by NMR spectroscopy.

X-ray Analyses of 4a−c and **5a−e**. The reflections were collected with an Enraf-Nonius CAD4 diffractometer (Mo Kα radiation, graphite monochromator, $\omega-2\theta$ scan). Intensities were corrected for Lorentz and polarization effects. The structures were solved by direct methods (MULTAN[29]). The structural parameters of the non-hydrogen atoms were refined anisotropically, and the parameters of the hydrogen atoms were refined isotropically according to a full-matrix least-squares technique (refinement on F^2). The hydrogen atoms of the tertiary butyl groups of **5d** were calculated and were fixed in the refinement. Calculations were carried out with the MolEN program system.[30] Crystallographic data are provided as Supporting Information.

Acknowledgment. Our work was supported by the Deutsche Forschungsgemeinschaft (SFB 247), the Fonds der Chemischen Industrie, and the BASF Aktiengesellschaft in Ludwigshafen. J.R. thanks the Studienstiftung des Deutschen Volkes for a Ph.D. fellowship.

Supporting Information Available: Figures showing molecular structures of **4c**, **5b−e**, complete Scheme 2, low-temperature ^{13}C NMR spectrum of **4b** at 183 K, and ^{13}C and ^1H NMR spectra of the dihydrochlorides and dideuteriochlorides of **5c** and a table of crystallographic data for **4a**,**c** and **5a−e** (15 pages). See any current masthead page for ordering and Internet access instructions.

JA9628258

(29) Main, P.; Fiske, S. J.; Hull, S. E.; Lessinger, L.; Germain, G.; Declercq, J.-P.; Woolfson, M. M. *MULTAN 11/82*; University of York, England, 1982.

(30) Fair, C. K. *MolEN*; Enraf-Nonius: Delft, The Netherlands, 1990.